

Supplementary Materials for

The coupling between auditory and motor cortices is rate-restricted: Evidence for an intrinsic speech-motor rhythm

M. Florencia Assaneo and David Poeppel

Published 7 February 2018, *Sci. Adv.* **4**, eaao3842 (2018)

DOI: 10.1126/sciadv.aao3842

This PDF file includes:

- fig. S1. Behavioral results.
- fig. S2. Functional localizations.
- fig. S3. PLV between auditory cortices and speech envelope.
- fig. S4. Synchronization between auditory and motor cortices.
- fig. S5. Power profiles for auditory and motor cortices.
- fig. S6. PLV between LA and RA areas.
- fig. S7. A simple neural model replicates behavioral results.
- fig. S8. A linear model does not replicate the auditory-motor synchronization pattern.

SUPPLEMENTARY MATERIALS

Behavioral performance

We investigated the performance of the individuals on the syllable detection task across the different syllable rate conditions (fig. S1). For all conditions, the performance is above chance (Wilcoxon signed rank test $p < 0.01$, FDR-corrected) and a Kruskal-Wallis test reveals no significant difference across conditions ($\chi^2(4) = 4.6$, $p = 0.32$). This result suggests that the synchronization between areas does not imply a benefit for perception. However, since the present study focuses on exploring the synchronization as a function of the syllable rate, regardless of its functional role, the behavioral task was designed to maintain the individual's attention on the stimuli - not to explore perception. Further work would be needed to assess the implications of the auditory-motor synchronization on perception.

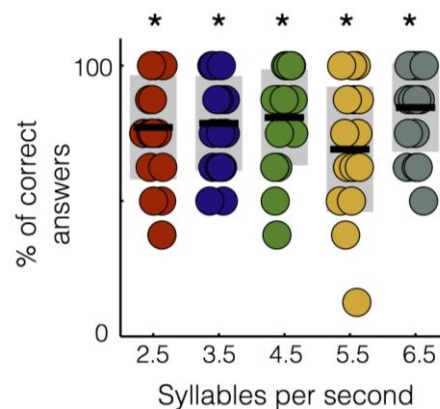


fig. S1. Behavioral results. Performance as a function of the syllable rate condition. Dots: individual participants. Black lines: mean across participants; shadowed region is standard deviation. Asterisks: significant difference from chance (Wilcoxon signed rank test $p < 0.01$, FDR-corrected). Colors identify the different conditions (red: 2.5, blue: 3.5, green: 4.5, yellow: 5.5 and dark gray: 6.5 syllables per seconds).

Functional localizations

We used source reconstruction techniques (MNE) to generate a reliable localization of bilateral auditory and speech-motor areas for each participant. The areas were localized in participant's native space, using each participant's structural magnetic resonance image (MRI).

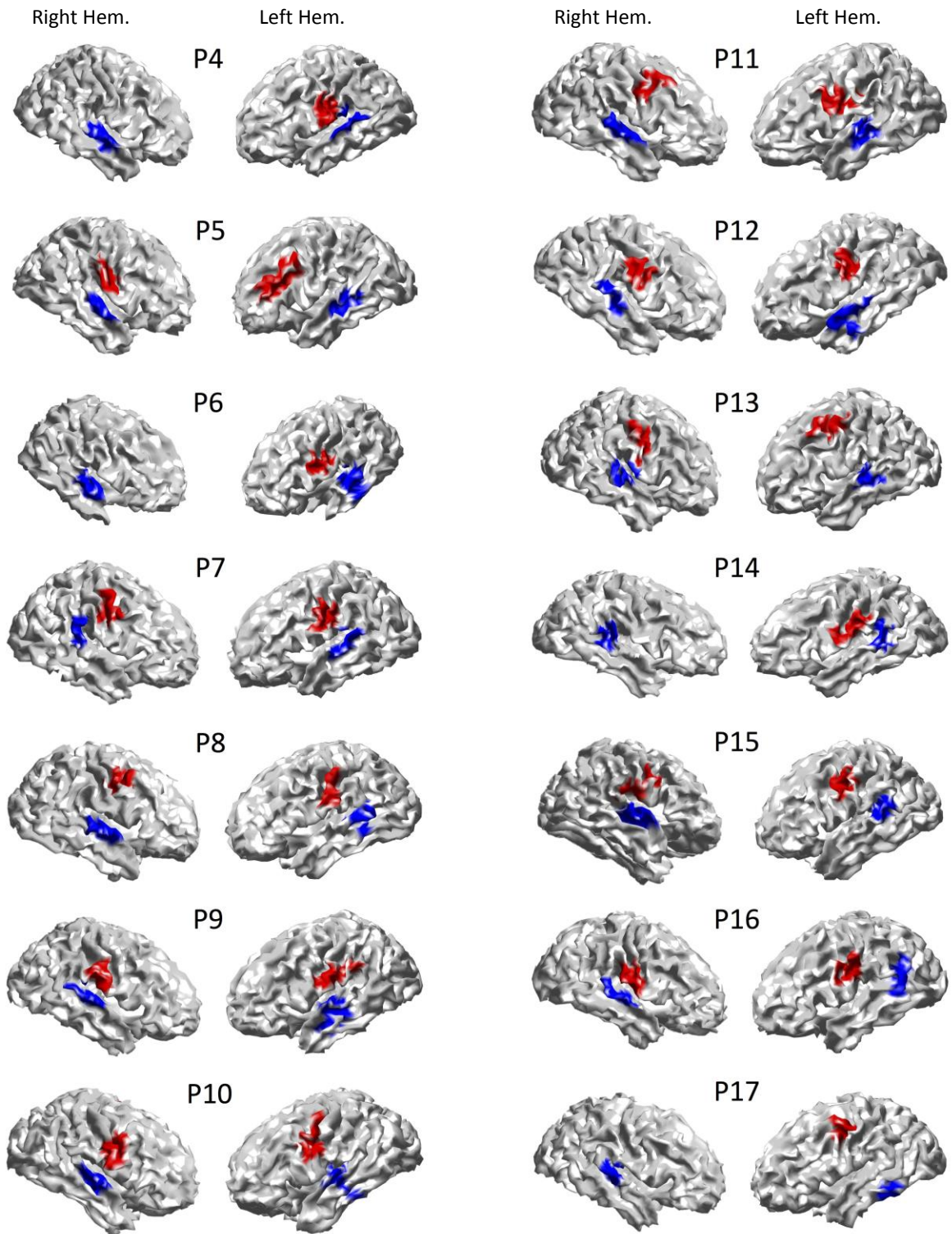


fig. S2. Functional localizations. Speech-motor (red) and auditory (blue) regions for the participants not displayed in the main text.

Activity in auditory cortices synchronizes to the speech envelope across rates

First, we calculated the PLV between auditory time series from each hemisphere and the speech envelope. Then, we computed the mean PLV, per condition and subject, around the perceived syllable rate (fig. S3). For all conditions and hemispheres, this last value showed an increment from baseline (Wilcoxon signed rank test $p < 0.002$, FDR-corrected). The mean PLV for the left auditory cortex showed no significant difference across conditions (Kruskal-Wallis test: $\chi^2(4) = 5.9$, $p = 0.21$); that was not the case for the right hemisphere ($\chi^2(4) = 10.3$, $p = 0.04$). However, a post-hoc analysis comparing the central condition (4.5 syllables per second) against all others showed no statistical differences (Wilcoxon signed rank test FDR corrected $p_{4.5|2.5} = 0.25$, $p_{4.5|3.5} = 0.3$, $p_{4.5|5.5} = 0.36$, $p_{4.5|6.5} = 0.25$).

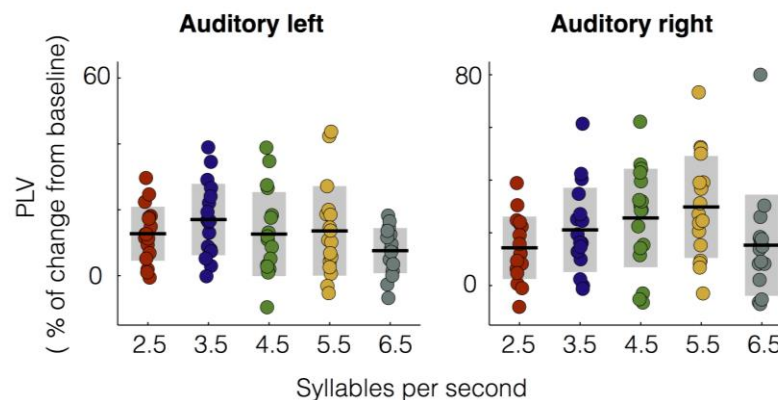


fig. S3. PLV between auditory cortices and speech envelope. Mean PLV around the syllable rate of each condition (syll. rate ± 0.5 Hz). The dots represent individual subjects, black lines the mean across subjects and the shadowed region the standard deviation of the data (red: 2.5, blue: 3.5, green: 4.5, yellow: 5.5 and dark gray: 6.5 syllables per seconds).

Synchronization between auditory and motor cortices reveals a preferred rate

We computed the contralateral PLVs (right motor - left auditory and left motor - right auditory) and averaged across trials within the same condition, and subjects. For both combinations of regions, a peak emerged at the frequency corresponding to the syllable rate for the lower rate conditions. However the enhancement of the PLV remains significant just for the central condition (fig. S4A, Wilcoxon signed rank test $p < 0.03$, FDR corrected). We also computed the mean PLV, per condition and subject, around the syllable rate and found that there is a significant difference across conditions (left motor - right auditory: $\chi^2(4) = 11.69$, $p = 0.02$ right motor - left auditory: $\chi^2(4) = 14.85$, $p = 0.005$ Kruskal-Wallis test). The mean PLV shows the same pattern as the average across region combinations: an enhancement of the synchronization for the central condition (fig. S4). For the left motor - right auditory synchronization, a post-hoc analysis comparing the central condition against all others revealed a significant difference between conditions (Wilcoxon signed rank test $p < 0.03$ FDR corrected). That was not the case for the right motor - left auditory PLV where the central condition was not significantly different from its the

neighboring conditions (Wilcoxon signed rank test $p_{4.5|3.5}=0.068$ $p_{4.5|5.5}=0.068$ $p_{4.5|2.5}=0.016$ $p_{4.5|6.5}=0.016$ FDR corrected).

In order to test the robustness of the previous result, we repeated the analysis using a different measure of synchronization: the debiased weighted phase lag index square estimator (wPLI). This index is less sensitive to crosstalk than PLV, but is blind to synchronization at near-zero phase differences (49). The synchronization computed using wPLI (see Materials and Methods) confirms an enhancement for the auditory motor coupling for the 4.5 syllables per second condition. The wPLI for this condition displays a significant increment from baseline for frequencies around the corresponding to the syllable rate (fig. S4B, Wilcoxon signed rank test $p<0.03$, FDR corrected). We also computed the mean PLV, per condition and subject, around the syllable rate and found that there is a significant difference across conditions (left motor - right auditory: $\chi^2(4)=10.69$, $p=0.03$ right motor - left auditory: $\chi^2(4)=9.73$, $p=0.045$ Kruskal-Wallis test). For the left motor - right auditory synchronization, a post-hoc analysis comparing the central condition against all others revealed a significant difference between conditions with exception of the 3.5 syllables per second one (Wilcoxon signed rank test $p_{4.5|2.5}=0.0016$ $p_{4.5|3.5}=0.33$ $p_{4.5|5.5}=0.011$ $p_{4.5|6.5}=0.0026$). That was not the case for the right motor - left auditory wPLI where the central condition was not significantly different from the two higher ones (Wilcoxon signed rank test $p_{4.5|2.5}=0.017$ $p_{4.5|3.5}=0.032$ $p_{4.5|5.5}=0.11$ $p_{4.5|6.5}=0.17$).

We computed the spectrum content for each cortical area and condition; and investigated how it changes as compared against baseline. We found a power enhancement around the corresponding syllable rate (fig. S5). A post hoc analysis comparing the central condition peak against all others, revealed a difference only from the 6.5 syllable rate condition in both regions (Wilcoxon signed rank test: Motor: $p_{4.5|2.5}=0.44$ $p_{4.5|3.5}=0.44$ $p_{4.5|5.5}=0.1$ $p_{4.5|6.5}=0.004$; Auditory: $p_{4.5|2.5}=0.8$ $p_{4.5|3.5}=0.8$ $p_{4.5|5.5}=0.9$ $p_{4.5|6.5}=0.005$ FDR corrected). However, because of the contiguity of our regions of interest and the space widespread of the MEG recordings, it is hard to isolate the contribution of each region's activity on each power spectrum profile.

To examine whether the observed synchronization pattern is restricted to the interaction between motor and auditory regions, we computed the PLV between auditory regions across hemispheres. This PLV showed a peak at the frequency corresponding to the syllable rate. The enhancement of the PLV around the heard syllable rate remains significant for all conditions with exception of the central and the last one (fig. S6, Wilcoxon signed rank test $p<0.03$, FDR corrected). However, the mean PLV, per condition and subject, around the syllable rate showed no significant difference across conditions as revealed by a Kruskal-Wallis test ($\chi^2(4)=3.31$, $p=0.51$).

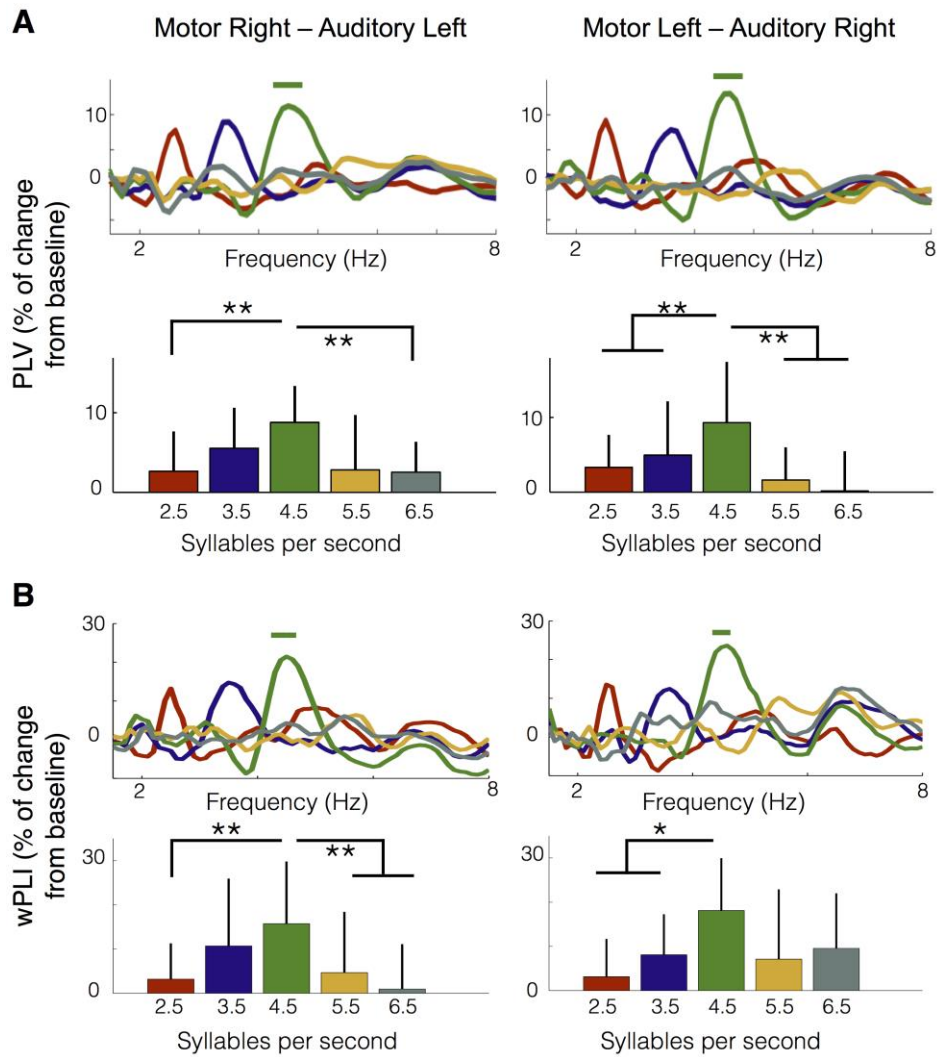


fig. S4. Synchronization between auditory and motor cortices. The upper panels display the increment from baseline of the synchronization between contralateral regions, as a function of frequency (red: 2.5, blue: 3.5, green: 4.5, yellow: 5.5 and dark gray: 6.5 syllables per seconds). Straight lines on top: significant increment from baseline (Wilcoxon signed rank test $p < 0.03$, FDR-corrected). Lower panels: the mean synchronization around the syllable rate of each condition (syll. rate ± 0.5 Hz). Double asterisk: $p < 0.03$ Wilcoxon signed rank test, FDR corrected. Single asterisk: $p < 0.05$ Wilcoxon signed rank test, uncorrected. **(A)** Results obtained using PLV. **(B)** Results obtained using wPLI.

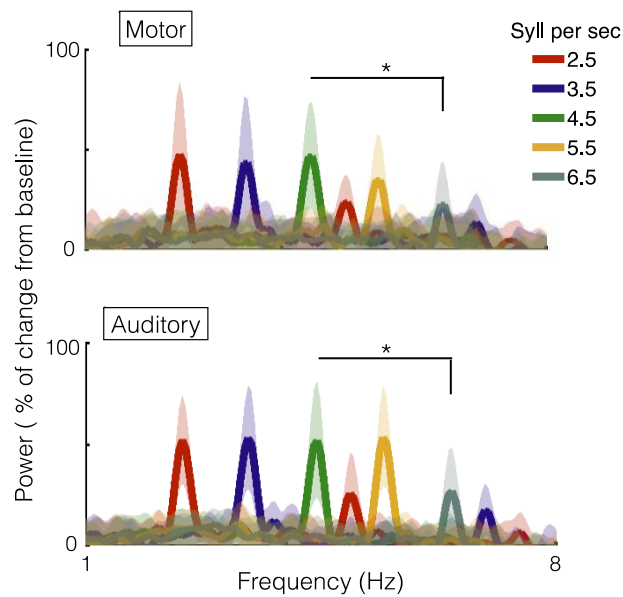


fig. S5. Power profiles for auditory and motor cortices. Percent of change from baseline of the power spectrums of each condition, averaged across subjects. The spectrums were obtained applying the fast fourier transform on the stimuli and baseline time window (red: 2.5, blue: 3.5, green: 4.5, yellow: 5.5 and dark gray: 6.5 syllables per seconds; shaded regions indicate the standard deviation of the data). Upper panel: motor areas; lower: auditory. The asterisk stands for significant difference between peaks (Wilcoxon signed rank test $p < 0.05$ corrected for false discovery rate).

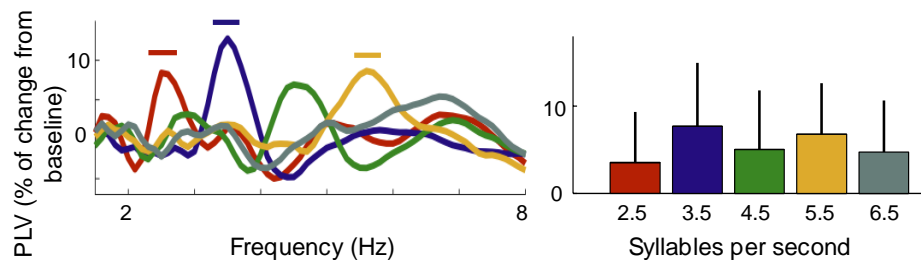


fig. S6. PLV between LA and RA areas. Left panel: Increment from baseline of PLV as a function of frequency, average across subjects. The straight lines at the top indicate a significant increment from zero (Wilcoxon signed rank test $p < 0.03$, FDR-corrected). Right panel: Mean PLV around the syllable rate of each condition (syll. rate ± 0.5 Hz). No significant difference across conditions.

A simple neural model successfully accounts for auditory-motor synchronization

One well-known psychophysical result is that when participants speak under delayed auditory feedback conditions (hearing themselves speak, with a delay inserted), their syllable rate is diminished (30,50). A neural model for the temporal dynamics of the sensorimotor integration of speech should be able to reproduce this

behavior. A first order approximation to reproduce this experimental condition would be assuming that the speech envelope is proportional to the motor cortex activity. Since the speech envelope entrains the auditory cortex, it follows that the auditory activity is proportional to the motor output with a given delay T (fig. S7). We explored the output of the model for different delays, finding that the fundamental frequency of the oscillations decreases while increasing the delay, in agreement with the experimental results. Moreover, the simulations closely follow previous experimental results (fig. S7) using delayed auditory feedback.

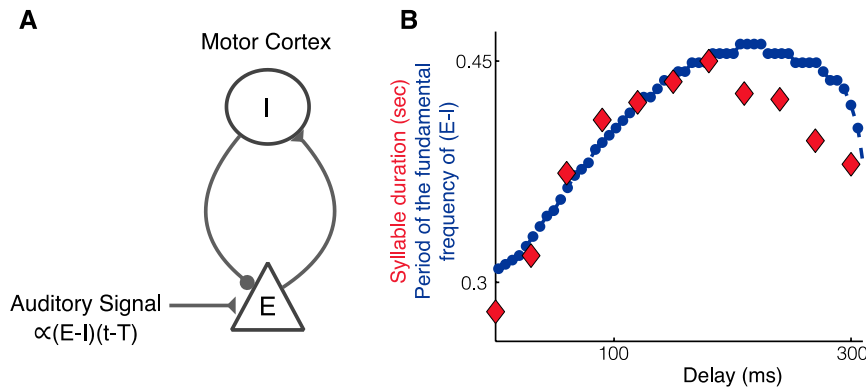


fig. S7. A simple neural model replicates behavioral results. (A) Schematic illustration of the neural model: motor cortex modeled through a set of Wilson-Cowan equations representing an inhibitory-excitatory network, the excitatory population receives the auditory cortex activity as input. (B) Numerical simulation replicating the delayed auditory feedback condition. Red dots: previously observed behavioral results(30). Blue line: period of the fundamental frequency of the output of the model as a function of the delay T . Auditory signal was set as $0.7[E(t - T) - I(t - T)]$; the other parameters were fixed at the same value as in the numerical simulations replicating the MEG experiment with exception of the basal inputs: $\rho_E=2.6$, $\rho_I=3.8$.

Finally, we repeated the numerical simulation representing the motor areas with a linear model driven by the auditory activity. Here, just one neuronal population, that exhibits periodic activity, describes the motor regions. The model is described by Equation S1; where M represents the motor activity, b is a damping factor, ω_0 is the harmonic frequency, κ represent the strength of the interaction and A the auditory cortical activity

$$\frac{d^2M}{dt^2} = -b \frac{dM}{dt} - (2\pi\omega_0)M + \kappa A \quad (\text{S1})$$

The parameters mirror the previous model: $\kappa=0.5$, $\omega_0=4.5$, $b=7$ and A is represented by Equation 3. Such a system is not capable of generating its own rhythm and will faithfully follow every forcing frequency. However, the amplitude of the response will increase when the external force approximates the harmonic frequency of the system. Once again, the whole MEG dataset for one participant was numerically simulated and submitted to the same analyses as the experimental data. The PLVs between the auditory and motor simulated time series,

averaged across trials of the same rate, are displayed in the left panel of fig. S8. For all five rate-conditions, the PLV shows a significant increment from baseline at the frequency corresponding to the syllable rate (Wilcoxon signed rank test $p < 0.03$, FDR-corrected). A Kruskal-Wallis test reveals no significant difference across conditions for the mean PLV around the condition rate (right panel of fig. S6; $\chi^2(4) = 4.19$, $p = 0.38$).

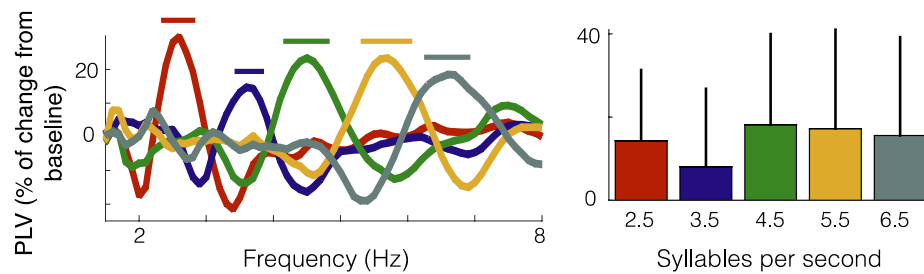


fig. S8. A linear model does not replicate the auditory-motor synchronization pattern. Numerical simulations submitted to the same analyses as the experimental dataset. Left panel: PLVs between the auditory and motor simulated time series, averaged across trials of the same rate. Straight lines: significant increment from baseline (Wilcoxon signed rank test $p < 0.03$, FDR-corrected). Right panel: Mean PLV around the syllable rate of each condition (syll. rate ± 0.5 Hz). No significant difference across conditions. Colors identify the different conditions (red: 2.5, blue: 3.5, green: 4.5, yellow: 5.5 and dark gray: 6.5 syllables per seconds).